POLITECNICO
MILANO 1863

SCUOLA DI INGEGNERIA INDUSTRIALE
E DELL'INFORMAZIONE

Executive Summary of the Thesis

Wheel-rail interaction models for rail corrugation monitoring through axlebox acceleration measurements

Laurea Magistrale in Mechanical Engineering - Ingegneria Meccanica

Author: Laurens Lanzillo

Advisor: Prof. Egidio Di Gialleonardo

Co-advisors: Ing. Leonardo Faccini, Ing. Claudio Somaschini

Academic year: 2021-2022

1. Introduction

Rail corrugation is a degradation phenomenon that is present in most of railway networks. It consists of a quasi-periodic irregularity of the rail running surface, having amplitudes ranging up to a few tenths of a millimeter. These irregularities can interact with the wheels passing over it, causing high dynamic loads between wheel and rail to be exchanged. These loads can in turn produce damage in the tracks or the rolling stock or give birth to unwanted ground-borne vibrations. The feedback loop behind corrugation growth has been described by Grassie et al. in [1].

The objective of this thesis is the development of an algorithm for the identification and monitoring of rail corrugation growth using axlebox acceleration measurements taken from an instrumented trainset in a section of the subway network of Milan. The irregularity estimation procedure is based on the state of the art present in literature [2]. Different models for the analysis of wheel-rail interaction in the frequency domain are derived in order to compute the measurement system transfer function. The measurement system transfer functions obtained by these models are then used to process acceleration data and reconstruct the rail roughness profiles.

The algorithm is validated by means of corrugation measurements made on the site of the subway network under analysis using a specialized diagnostic draisine. The robustness of the algorithm to changes in the measurement conditions is tested. Finally, the possibility of monitoring corrugation evolution over time is investigated by analyzing acceleration acquisitions taken over a period of three months.

2. Axlebox accelerometer system layout

Data used for this thesis is acquired by a series of sensors placed in the axleboxes of a trailer bogie of a *Meneghino* trainset operated by the transit company *Azienda Trasporti Milanesi* along Milan underground network. Acceleration measurements are taken from the set of sensors in correspondence to the leading wheelset of the bogies - according to the travel direction. Since accelerometers do not directly measure the rail irregularity, the Transfer Function between rail irregularity and axlebox acceleration is computed by implementing three different models of the wheel-rail interaction of increasing com-

plexity. Once these functions are computed, the rail profile can be reconstructed starting from the acquired acceleration measurements.
At first, raw data (sampled at a frequency of 1000 Hz) is filtered and the periodic component associated with wheel roughness is removed, as suggested by Carrigan in [3]. The irregularity spectra can be obtained by processing the filtered acceleration data with the measurement system transfer function in the frequency domain and then applying an inverse Fourier transform to the results. The reconstructed rail profiles are processed to obtain synthetic indexes which measure roughness severity in selected wavelength intervals, as stated by the Standard EN 13231-3:2012 [4].
The measurement system transfer functions are computed starting from the receptances of the wheelset and the track.
The rail is modeled according to Faccini et al. in [6]. Its behavior is computed analytically by means of an infinite Timoshenko beam lying on a double layer, continuous support. The model is validated by comparing it to the results of experimental tests performed in [6] and used to extract rail vertical and lateral receptances.
Wheelset receptances are computed by means of a modal model whose mode shapes have been obtained through a Finite Element simulation and whose eigenfrequencies are adjusted according to the results of an experimental modal identification campaign. The experimental campaign is described in the following section.

3. Experimental modal analysis of the wheelset

The experimental modal analysis aims at identifying the modal parameters of the wheelset. An trailer wheelset of a *Meneghino* trainset is instrumented using a series of accelerometers and subjected to a series of impact tests. In order to reproduce the conditions of a free wheelset and ease the modeling of constraints, the wheelset was suspended from the laboratory's bridge crane and insulated from vibrations by using two sets of springs.
The Frequency Response Functions between the input forces and output accelerances are estimated by using power spectral density and are used to identify natural frequencies and damping ratios of the wheelset which are exposed in Table 1. The modal frequencies are paired with

f (Exp.)	f (FEM)	Damping ratio
71 Hz	72 Hz	0.141%
72 Hz	71 Hz	0.428%
128 Hz	119 Hz	0.098%
195 Hz	176 Hz	0.129%
221 Hz	195 Hz	0.052%
270 Hz	305 Hz	0.034%
286 Hz	305 Hz	0.424%
322 Hz	380 Hz	0.043%
425 Hz	419 Hz	0.011%

Table 1: Identified modal frequencies.

the modal shapes obtained by a FEM analysis of the wheelset and validated against the experimental results. The resulting modal model is used to compute the receptances of the wheelset in the points and directions highlighted by Figure 3,i.e. the two wheel contact points and the two axleboxes. Finally, the modal model results

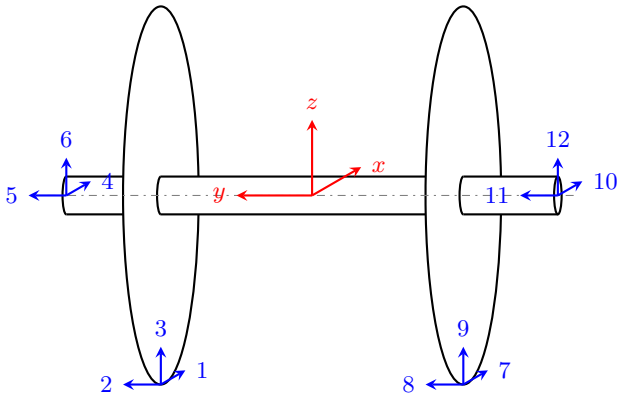

Figure 1: Receptances reference system.

are compared to the experimental Frequency Response Functions of the wheelset acquired in the experimental campaign. Figure 4 shows how the modal model is able to correctly simulate the actual behavior of the wheelset in the frequency range of interest (0-500 Hz).

4. Models for wheel-rail interaction

In order to derive the measurement system transfer function, the interaction between the vehicle and track needs to be modeled. Literature suggests that, for the frequency range of corrugation monitoring, it is sufficient to take

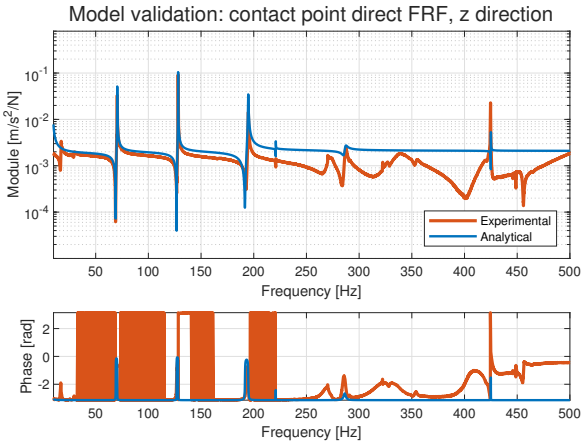

Figure 2: Contact point direct FRF validation, vertical direction.

into account the dynamic of the wheelset and the tracks, while neglecting the rest of the vehicle [5]. Wheel-rail interaction is schematized by Figure 3. The dynamic force between wheel and rail is aligned in the normal directions n_L and n_R, inclined with respect to the vertical direction by angles θ_L and θ_R respectively. Contact between wheel and rail is modeled through a linearized Hertzian spring of stiffness K_H. Three different approaches are analyzed when modeling the wheel-rail interaction, with the following subsections briefly describing their main features.

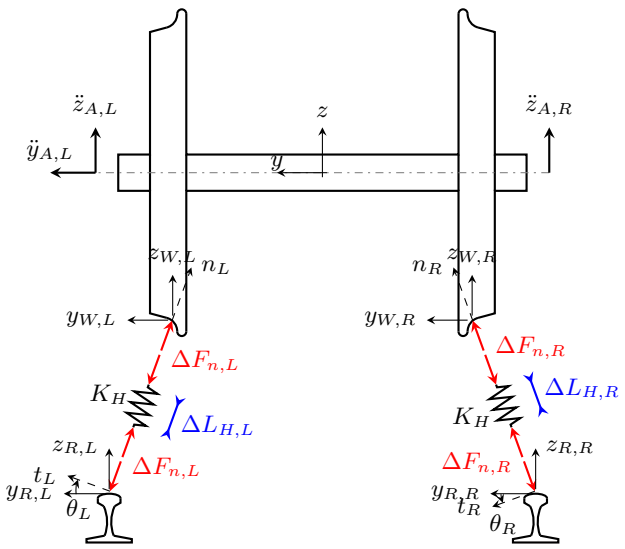

Figure 3: Irregularity detection algorithm layout

4.1. Half wheelset approach

The first interaction model is based on a state-of-the-art model of a flexible half-wheelset which neglects the dynamic coupling between the two wheels. Wheel-rail interaction is assumed to be aligned in the vertical direction, therefore $\theta = 0$. The relationship between the vertical irregularity and the contact force $\Delta F_n \approx \Delta F_Z$ is:

$$z_{irr} = (A_{3,3} + A_{R,Z} + K_H)\Delta F_Z \tag{1}$$

where $A_{R,Z}$ is the rail receptance in the vertical direction and $A_{3,3}$ (according to the notation presented in Figure 3) is the contact point direct vertical receptance. The transfer function between irregularity and axlebox acceleration can therefore be written as:

$$z_{irr} = \frac{A_{3,3} + A_{R,Z} + K_H}{-\Omega^2 A_{3,6}} \ddot{z}_A \tag{2}$$

where $A_{3,6}$ is the vertical receptance between the contact point and the axlebox.

4.2. Vertical dynamic of the full wheelset

The second approach introduces the full dynamic of the wheelset and therefore the coupling between the two sides, creating a multi-input, multi-output model. Forces and displacements are still considered to act in the vertical direction only. The receptance matrix between the two vertical irregularities $[z_{irr,L} \quad z_{irr,R}]^\mathsf{T}$ and the contact forces $[\Delta F_{Z,L} \quad \Delta F_{Z,R}]^\mathsf{T}$ is described by the receptance matrix A_W being:

$$[A_W] = \begin{bmatrix} A_{3,3} + A_{R,Z} + \frac{1}{K_H} & A_{3,9} \\ A_{9,3} & A_{9,9} + A_{R,Z} + \frac{1}{K_H} \end{bmatrix}$$

Similarly, the relationship between the contact forces and the vertical displacements of the axleboxes can be mediated by the matrix A_B represented as:

$$\begin{bmatrix} z_{A,L} \\ z_{A,R} \end{bmatrix} = [A_B]\underline{\Delta F} = \begin{bmatrix} A_{6,3} & A_{6,9} \\ A_{12,3} & A_{12,9} \end{bmatrix} \begin{bmatrix} \Delta F_{Z,L} \\ \Delta F_{Z,R} \end{bmatrix}$$

The total transfer function between the rail irregularities and the axleboxes accelerations can therefore be written as:

$$\begin{bmatrix} z_{irr,L} \\ z_{irr,R} \end{bmatrix} = -[A_W]\frac{1}{\Omega^2}[A_B]^{-1} \begin{bmatrix} \ddot{z}_{A,L} \\ \ddot{z}_{A,R} \end{bmatrix} \tag{3}$$

4.3. Vertical and lateral dynamics of the wheelset

The effect of the inclination of the wheel-rail contact planes is subsequently added to the third and last model, thereby introducing the effect of the lateral dynamics of the full wheelset. Wheel and rail exchange a normal force F_n perpendicular to the contact plane. The contact problem is therefore written along the normal direction n, while the receptances matrixes (which now account for the terms in directions y and z) are written according to the reference system of the wheelset. The passage between these references system is assured by means of the change-of-basis matrix $[\Lambda(\theta_L, \theta_R)]$ according to:

$$\underline{v}_{y,z} = [\Lambda(\theta_L, \theta_R)]\underline{v}_{t,n} \tag{4}$$

Where $\underline{v}_{y,z} = [v_{y,L} \quad v_{z,L} \quad v_{y,R} \quad v_{z,R}]^\mathsf{T}$ is a vector containing forces or displacements on the two contact points according to the wheelset reference system and $\underline{v}_{t,n} = [v_{t,L} \quad v_{n,L} \quad v_{t,R} \quad v_{n,R}]^\mathsf{T}$ is the corresponding vector oriented along the reference system of the contact plane. The diagonal rail receptance matrix $[A_R]$ introduction allows computing the measurement system transfer function as:

$$\underline{n}_{irr} = -\left([\Lambda]^\mathsf{T}[A_W][\Lambda] + [\Lambda]^\mathsf{T}[A_R][\Lambda] + [A_{H,n}]\right) \frac{1}{\Omega^2}\left(-[A_B][\Lambda]\right)^{-1}\underline{\ddot{X}}_A \tag{5}$$

Where $\underline{\ddot{X}}_A$ is the vector of axlebox accelerations and $\underline{n}_{irr}$ is the rail irregularity vector.

5. Results

The transfer functions obtained by the three aforementioned approaches are employed to reconstruct the moving average of peak-to-peak amplitudes of the irregularity profile of a right turn of a section of Milan underground network. The curve under analysis presents corrugation on its low rail and it is covered by the instrumented trainset multiple times per day. The results of the irregularity reconstruction of multiple runs can therefore be averaged: this is found to improve the robustness and accuracy of results. The results of the analysis are represented in Figure 4 alongside the irregularity profile of the curve taken by a specialized diagnostic draisine.

All three models show similar performance in the wavelength band 30-100 mm. An analysis of the results in the wavelength band 100-300 mm shows that, when the half wheelset model is considered, the proposed methodology tends to overestimate corrugation amplitude in this wavelength interval. The use of the model accounting for the vertical dynamic of the full-wheelset instead results in the peak-to-peak amplitude profiles being equal on the two rails and therefore producing unusable data. The algorithm using the model which accounts for both vertical and lateral dynamics is able to correctly discern the side at which corrugation appears and obtain a more accurate estimation of its amplitude. In the analysis of this curve, the contact angles are calculated by using a multibody simulation of the train negotiating it. However, the difficulties embedded in the correct computation of the two contact angles along the whole line complicate the implementation of this methodology.

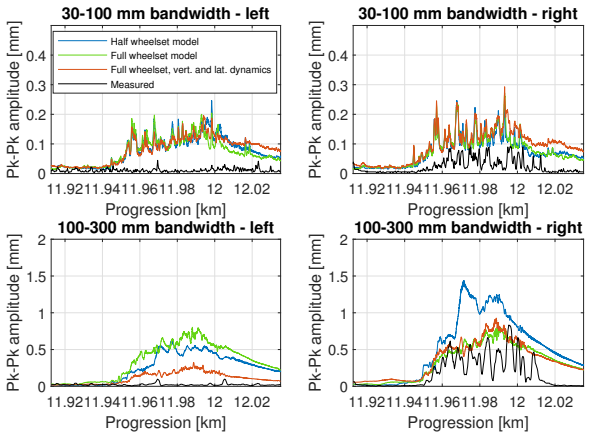

Figure 4: Comparison of the three models' results.

The robustness of the measurement system to uncertainties is then checked. Several variables can in fact affect the reconstruction of irregularity, such as environmental conditions, effects of wear and wheel reprofiling, etc... In order to simulate these uncertainties, a series of modified transfer functions are constructed, each obtained by randomly varying the modal frequencies and damping ratios of the nominal one. The modified transfer functions process an ac-

celerometer signal which reproduces the effects on the measurement system of a rail profile having uniform irregularity at all wavelengths. The standard deviation of the reconstructed profiles spectra is then computed and represented in Figure 5.

A significant dispersion in the results is observed at frequencies corresponding to the natural frequencies of the wheel-rail dynamic. These results have significant impacts on the reliability of the reconstructed rail profiles, since small variations in the measurement conditions can significantly affect the measurement system output. This is worsened by corrugation spatial wavelengths being usually associated to the natural frequencies of the system. A similar analysis

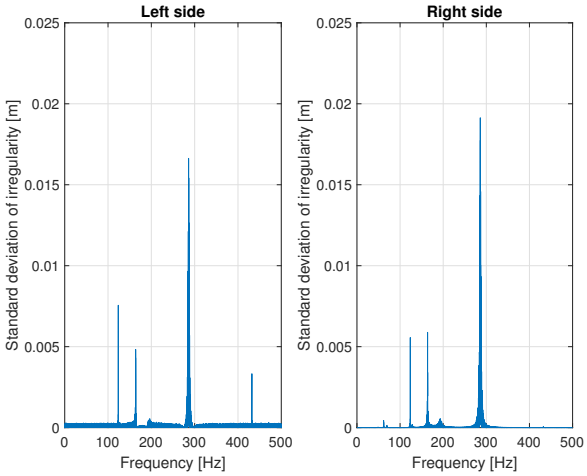

Figure 5: Spectral standard deviation.

is performed by using the same set of modified transfer functions to reconstruct the irregularity profiles of the line section under analysis. Figure 6 shows the average peak-to-peak amplitude profile (black line) and the boundaries of the interval corresponding to a confidence level of 95% of the results. The results highlight the large dispersion that small changes in measurement conditions can cause on the final results.

Since the frequency at which the irregularity excites wheel-rail dynamics depends on its wavelength λ and on the train speed v through the relationship:

$$f = \frac{\lambda}{v} \tag{6}$$

Performances of the measurement system intrinsically depend on the train speed. Corrugation wavelengths can therefore correspond to peaks in the measurement system transfer function or not depending on v.

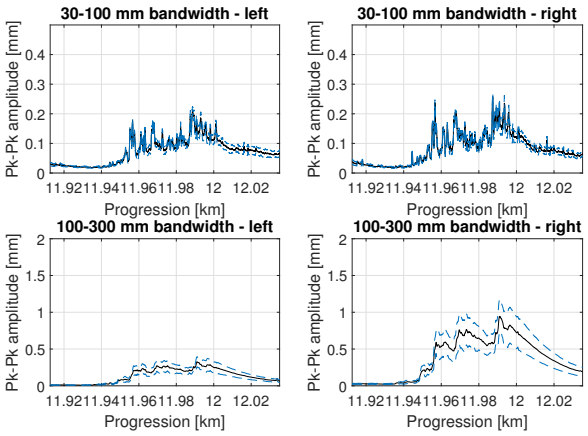

Figure 6: Confidence intervals of the reconstructed rail irregularity profile.

The possibility of monitoring the evolution of rail corrugation over time is investigated. In order to do so, a set of days are selected to cover the period between two consecutive grinding operation over the span of three months. For each day under analysis, the results coming from all the runs recorded by the instrumented trainset are averaged. Results of this analysis are highlighted in Figure 7. For reference, a series of measurements taken the day after the final grinding operation are averaged (dashed line). The reconstructed moving average of peak-to-peak amplitude profiles are effective in correctly tracking corrugation growth over time and the subsequent successful rail grinding operation, suggesting the possibility of using these models to track the effectiveness of corrugation removal.

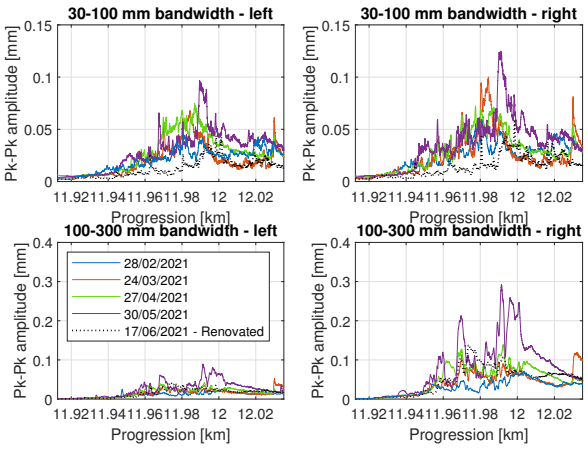

Figure 7: Roughness evolution over time.

6. Conclusions

In this work, an algorithm for the identification and monitoring of rail corrugation growth using axlebox acceleration measurements taken from an instrumented trainset is developed. Different models for the wheel-rail interaction are therefore formulated in order to compute the transfer function between rail irregularity and axlebox acceleration measurements. The models' performances are investigated using data coming from instrumented trainsets and their robustness is checked. It is shown that the measurement system's results are highly susceptible to variations in the measurement conditions. Averaging multiple runs is found to be a possible way to improve robustness in the results, a solution eased by the fact that the instrumented trainset covers the entire subway line multiple times per day. Finally, the algorithm is demonstrated to be capable of monitoring the growth of corrugation over time and the success of rail grinding operations in removing irregularities. An investigation into the creation of an irregularity measurement algorithm that is independent of train speed could be a possible future development of this work.

7. Bibliography

References

[1] S. L. Grassie and J. Kalousek. Rail corrugation: characteristics, causes and treatments. *Proceedings of the Institution of Mechanical Engineers, Part F: Journal of Rail and Rapid Transit*, 207(1):57–68, 1993.

[2] E. Di Gialleonardo, J. Karaki, L. Faccini, C. Somaschini, M. Bocciolone, and A. Collina. Continuous monitoring of rail corrugation growth using an in-service vehicle. In Anna Orlova and David Cole, editors, *Advances in Dynamics of Vehicles on Roads and Tracks II*, pages 158–167. Springer International Publishing, 2022. doi: 10.1007/978-3-031-07305-2_17.

[3] T. D. Carrigan and J. P. Talbot. Use of flexible wheelset model, comb filter and track identification to derive rail roughness from axle-box acceleration in the presence of wheel roughness. In *Proceedings of 14th International Workshop On Railway Noise*, pages 232–239. INTEX, 2022.

[4] BS EN 13231-3:2012. standard, BSI Standard Publications.

[5] S. L. Grassie. Measurement of railhead longitudinal profiles: A comparison of different techniques. *Wear*, 191, 1996. ISSN 00431648. doi: 10.1016/0043-1648(95)06732-9.

[6] L. Faccini, J. Karaki, E. Di Gialleonardo, C. Somaschini, M. Bocciolone, and A. Collina. A methodology for continuous monitoring of rail corrugation on subway lines based on axlebox acceleration measurements. *Applied Sciences*, 13(6), 2023. ISSN 2076-3417. doi: 10.3390/app13063773.